Electron Spin Echo Envelope Modulation Spectroscopy Supports the Suggested Coordination of Two Histidine Ligands to the Rieske Fe–S Centers of the Cytochrome b_6f Complex of Spinach and the Cytochrome bc_1 Complexes of *Rhodospirillum rubrum*, *Rhodobacter sphaeroides* R-26, and Bovine Heart Mitochondria†

R. David Britt,*,‡ Kenneth Sauer, and Melvin P. Klein
Laboratory of Chemical Biodynamics, Lawrence Berkeley Laboratory, Berkeley, California 94720
David B. Knaff and Aidas Kriauciunas
Department of Chemistry and Biochemistry, Texas Tech University, Lubbock, Texas 79409
Chang-An Yu and Linda Yu
Department of Biochemistry, Oklahoma State University, Stillwater, Oklahoma 74078
Richard Malkin
Department of Plant Biology, University of California, Berkeley, California 94720
Received February 9, 1990; Revised Manuscript Received October 22, 1990

ABSTRACT: Electron spin echo envelope modulation (ESEEM) experiments performed on the Rieske Fe–S clusters of the cytochrome b_6f complex of spinach chloroplasts and of the cytochrome bc_1 complexes of *Rhodospirillum rubrum*, *Rhodobacter sphaeroides* R-26, and bovine heart mitochondria show modulation components resulting from two distinct classes of ^{14}N ligands. At the $g = 1.92$ region of the Rieske EPR spectrum of the cytochrome b_6f complex, the measured hyperfine couplings for the two classes of coupled nitrogens are $A_1 = 4.6$ MHz and $A_2 = 3.8$ MHz. Similar couplings are observed for the Rieske centers in the three cytochrome bc_1 complexes. These ESEEM results indicate a nitrogen coordination environment for these Rieske Fe–S centers that is similar to that of the Fe–S cluster of a bacterial dioxygenase enzyme with two coordinated histidine ligands [Gurbiel, R. J., Batie, C. J., Sivaraja, M., True, A. E., Fee, J. A., Hoffman, B. M., & Ballou, D. P. (1989) *Biochemistry 28*, 4861–4871]. The Rieske Fe–S cluster lacks modulation components from a weakly coupled peptide nitrogen observed in water-soluble spinach ferredoxin. Treatment with the quinone analogue inhibitor DBMIB causes a shift in the Rieske EPR spectrum to $g = 1.95$ with no alteration in the magnetic couplings to the two nitrogen atoms. However, the ESEEM pattern of the DBMIB-altered Rieske EPR signal shows evidence of an additional weakly coupled nitrogen similar to that observed in the spinach ferrodoxin ESEEM patterns.

In plant photosynthesis the membrane-bound cytochrome b_6f complex serves as an electron-transfer component between photosystem II and photosystem I (Ort, 1986). Plastoquinone is reduced to platoquinol by the reducing side of photosystem II. Plastocyanin is oxidized by the photooxidized reaction center pigment of photosystem I. The cytochrome b_6f complex couples the two-electron oxidation of plastoquinol to the single-electron reduction of plastocyanin. The electron transfer is accompanied by a transfer of protons from the outer to the inner surfaces of the thylakoid membrane. The cytochrome b_6f complex is also employed in cyclic electron flow around photosystem I. The membrane-bound cytochrome bc_1 complex serves a similar function in cyclic electron flow in anoxygenic photosynthetic bacteria (Dutton, 1986). In this case, electrons from quinol molecules are transferred to ferricytochrome c_2. Analogous cytochrome bc_1 complexes are involved in quinol-cytochrome *c* oxidoreductase activity in mitochondrial respiration (Rieske, 1976). In all cases, pairs of electrons from quinol molecules are transferred to metal centers that can be only singly reduced, and the electron transfer is coupled to translocation of protons through the membrane (Hauska et al., 1983; Hauska, 1986). Details of the functional mechanisms of these quinol-cytochrome *c* or plastocyanin oxidoreductases are not yet completely resolved. The Q cycle proposed by Mitchell (1975, 1976) serves as a basis for most current models, but other mechanisms have also been proposed (Wikström & Krab, 1980; Wikström et al., 1981). All of the oxidoreductases are of similar composition. Each contains inequivalent protoheme groups located in a single cytochrome *b* peptide, a single *c*-type cytochrome (cytochrome c_1 or *f*), and a single Rieske Fe–S center.

The Rieske Fe–S protein component was first discovered in the mitochondrial cytochrome bc_1 complex (Rieske et al., 1964). The Rieske Fe–S center has a high midpoint potential (approximately 285 mV in the cytochrome b_6f complex), and the reduced center gives rise to a characteristic EPR signal with *g* values of 1.76, 1.90, and 2.01. Shifts to larger *g* values can be induced in the Rieske Fe–S EPR signal by treatments with several halogenated quinone inhibitors (Malkin, 1982). Fe–S clusters in several other enzymes give rise to EPR spectra

† This work was supported by the Director, Office of Energy Research, Office of Basic Energy Sciences, Division of Energy Biosciences of the Department of Energy, under Contract DE-AC03-76SF00098, and the United States Department of Agriculture, Grant 85-CRCR-1-1847 (K.S. and M.P.K); by the National Science Foundation, Grant DMB-8806609, and the Robert A. Welch Foundation, Grant D-0170 (D.B.K.); and by the National Institutes of Health, Grants GM 30721 (C.-A.Y.) and GM 20571 (R.M.).
‡ Present address: Department of Chemistry, University of California, Davis, CA 95616.

0006-2960/91/0430-1892$02.50/0

that are very similar to those of the native Rieske Fe–S clusters in the oxidoreductases. Blumberg and Peisach (1974) considered the EPR spectra and their changes upon selenium substitution to indicate the presence of atoms less electron donating that sulfur in the Fe–S clusters of two such enzymes, cytochrome *c*-coenzyme Q reductase and 4-methoxybenzoate O-demethylase. The ligand-field model of Bertrand et al. (1985) suggested that the low average g values of Rieske type Fe–S clusters could arise from a large chemical inequivalence of the Fe^{2+} terminal ligands compared to the bridging sulfurs. However, compression of the Fe^{2+} site resulting in a change in ligand field symmetry from C_{2v} to D_2 could similarly result in a decrease of the average g values of an Fe–S cluster with only sulfur ligands.

Fee et al. (1984) isolated a protein from the thermophilic bacterium *Thermus thermophilus* that contains an Fe–S cluster with g values similar to those of the oxidoreductase Rieske clusters. Chemical analysis showed that this *T. thermophilus* Rieske protein contains four irons, four sulfides, and four cysteines. Furthermore, Mössbauer spectra obtained with ^{57}Fe-enriched protein samples determined the Fe–S clusters to be of the 2Fe–2S type. Together, the chemical composition analysis and the Mössbauer data indicated that the *T. thermophilus* protein contains two spectroscopically identical 2Fe–2S clusters, each with less than the complement of four cysteines observed in typical ferredoxin 2Fe–2S clusters. Analysis of the Mössbauer isomer shifts in comparison with results from other 2Fe–2S clusters suggested that non-sulfur ligands are coordinated to the Fe^{2+} site in the reduced cluster.

Cline et al. (1985) applied electron nuclear double resonance (ENDOR)[1] to the study of the *T. thermophilus* Fe–S complex and the "Rieske-type" Fe–S cluster of the phthalate dioxygenase enzyme from *Pseudomonas cepacia*. The X-band ENDOR results for both Fe–S clusters showed features in the 11–14 MHz range that were assigned to directly coordinated nitrogen nuclei with hyperfine coupling constants $A(^{14}N) \approx$ 26–28 MHz. Both Fe–S clusters also exhibited broad ENDOR features in the 4–5-MHz region. These transitions were tentatively assigned to a second class of coordinated nitrogen with $A(^{14}N) \approx 9$ MHz. ENDOR spectra of the Rieske center of yeast mitochondrial complex III (Tesler et al., 1987) were similar to those observed in the *T. thermophilus* Rieske protein and the phthalate dioxygenase enzyme. Electron spin echo envelope modulation results were also displayed for the *T. thermophilus* Rieske protein (Cline et al., 1985) and the complex III Rieske center (Tesler et al., 1987). Various low-frequency modulation components were observed, but rigorous analyses of the frequencies were not provided.

Gurbiel et al. (1989) recently published ENDOR spectra of the Fe–S center of the phthalate dioxygenase enzyme isolated from *P. cepacia* grown alternately from media with ^{14}N in natural abundance, ^{15}N-enriched media, ^{14}N media supplemented with ^{15}N-labeled histidine, and ^{15}N-enriched media supplemented with natural abundance ^{14}N-labeled histidine. These results provide a very different description of the nitrogen environment compared to that from the earlier ENDOR studies. The ENDOR spectrum obtained with the ^{15}N-enriched center shows a set of four transitions attributable to a pair of inequivalent ^{15}N nitrogen sites. The ENDOR studies of the auxotroph of *P. cepacia* grown on ^{15}N-labeled histidine added to natural abundance ^{14}N-containing media conclusively demonstrated that the two nitrogens observed in the ENDOR experiment belong to histidine residues. The ^{15}N ENDOR resonances appear to correspond to the low-frequency ^{14}N transitions discussed in the previous ENDOR papers (Cline et al., 1985; Tesler et al., 1987). Q-band ENDOR experiments demonstrated that the higher frequency resonances previously assigned to a strongly coupled nitrogen are in fact due to protons. Gurbiel et al. include analyses of the hyperfine coupling tensors for the ^{15}N-labeled phthalate dioxygenase Rieske center and the ^{14}N quadrupolar coupling tensors for the Rieske center isolated with natural abundance ^{14}N. The magnitude of the hyperfine couplings are taken as evidence that the two nitrogens are directly bound to the Fe–S cluster. The ^{14}N quadrupolar tensors are compared with those of the axially bound histidine nitrogen in aquometmyoglobin (Scholes et al., 1982). The results of these analyses of the ENDOR results, along with the previously described Mössbauer data on the *T. thermophilus* Rieske protein and EXAFS results on the Rieske Fe–S center of the phthalate dioxygenase enzyme (Tsang et al., 1989), led Gurbiel et al. to propose a model for the specific structure of the Fe–S complex, with two imidazoles from protein histidine residues completing a nearly tetrahedral coordination environment about the Fe^{2+} of the reduced cluster. By comparison with previous ENDOR results, they also suggest that this coordination geometry is present in all Rieske-type centers.

However, there have been several other coordination environments proposed for the Rieske centers of the oxidoreductase enzymes. Nitschke and Hauska (1987) performed ENDOR spectroscopy on the Rieske Fe–S center of the cytochrome b_6f complex and found no evidence for nitrogen ligands. This result led them to suggest that the Fe–S cluster in this complex is bound by only cysteine ligands. Powers et al. (1989) used the EXAFS technique to study the Rieske protein isolated from the cytochrome bc_1 complex of bovine heart mitochondria. The detailed analysis of the EXAFS data was taken to favor a coordination environment of 3.5 sulfur atoms and 0.5 nitrogen atoms per iron, corresponding to only one nitrogen ligand per 2Fe–2S cluster. However, they could not completely exclude the possibility of coordination of two nitrogen ligands to the cluster. All Rieske Fe–S proteins from cytochrome bc_1 or cytochrome b_6f complexes for which amino acid sequences are available have two conserved histidine residues and four conserved cysteine residues in a region near the C-terminus (Harnisch et al., 1985; Gabellini & Sebald, 1986; Schägger et al, 1987; Beckmann et al, 1987; Steppuhn et al, 1987; Kurowski & Ludwig, 1987). Gatti et al. (1989) examined the enzymatic activity and EPR spectra of a set of yeast mutants with single amino acid substitutions in the C-terminal end of the Rieske protein and presented a model where the two Fe atoms are coordinated by one histidine and three cysteine residues.

In this paper, we report the results of electron spin echo envelope modulation (ESEEM) studies of the Rieske Fe–S centers of the cytochrome b_6f complex of spinach and the cytochrome bc_1 complexes of bovine heart mitochondria, *Rhodospirillum rubrum*, and *Rhodobacter sphaeroides* strain R-26. The ESEEM results obtained at two distinct microwave excitation frequencies are analyzed to demonstrate the presence of two classes of ^{14}N nuclei magnetically coupled to the Rieske Fe–S clusters. The hyperfine and quadrupole couplings for the two classes of ^{14}N nuclei are determined from analysis of the ESEEM spectra. From the magnitudes of the superhyperfine couplings (A_1 = 4.6 MHz and A_2 = 3.8 MHz), we conclude that the two classes result from direct coordination

[1] Abbreviations: DBMIB, 2,5-dibromo-3-methyl-5-isopropylbenzoquinone; DMSO, dimethyl sulfoxide; ENDOR, electron–nuclear double resonance; ESEEM, electron spin echo envelope modulation; EXAFS, X-ray absorption fine structure; NQR, nuclear quadrupole resonance.

of nitrogen ligands to the Rieske Fe–S centers. Furthermore, the hyperfine and quadrupole coupling constants for the two classes are very similar to those derived from the ENDOR results on the Rieske center of the phthalate dioxygenase enzyme. We therefore conclude that a similar coordination of two histidines is indeed present in the Rieske cluster of the membrane-bound oxidoreductases of plant chloroplasts, photosynthetic bacteria, and mitochondria. The same coordination is observed for the Rieske center of the DBMIB-treated cytochrome b_6f complex, even though the EPR spectrum is dramatically altered by this treatment.

Experimental Procedures

Protein Isolation. The cytochrome b_6f complex was isolated from spinach chloroplast membranes by using octyl glucoside plus cholate by the procedure of Hurt and Hauska (1981) except that membranes were washed only once with 2 M NaBr and the phospholipids were omitted from the final sucrose gradient. The cytochrome bc_1 complex from *R. sphaeroides* R-26 was prepared by the method of Yu et al. (1984). Isolation of the cytochrome bc_1 complex from *R. rubrum* strain S1 was performed as described by Kriausiunas et al. (1989). The bovine heart mitochondrial cytochrome bc_1 complex was isolated by the method described by Yu and Yu (1980). EPR samples of each of the oxidoreductase complexes were prepared with final protein concentrations of approximately 70 μM in buffers containing 30% ethylene glycol. The Rieske Fe–S centers were reduced with addition of 100 mM stock solution of ascorbic acid to a final concentration of 2 mM. Spinach ferredoxin was isolated by the method described by Buchanan and Arnon (1971). The EPR sample was prepared with a protein concentration of approximately 500 μM in a buffer containing 30% ethylene glycol. The ferredoxin Fe–S centers were reduced by the addition of a stock solution of sodium dithionite to a concentration of 10 mM. Samples were placed in 3.8-mm-o.d. quartz EPR tubes and frozen in liquid nitrogen. The quinone analogue 2,5-dibromo-3-methyl-5-isopropylbenzoquinone (DBMIB) was purchased from Sigma Chemical Co. DBMIB treatment of the cytochrome b_6f Rieske centers was performed by the addition of 20 mM DBMIB in DMSO to the aforementioned cytochrome b_6f preparations before the addition of ascorbic acid. The final concentration of DBMIB in the preparations was approximately 2 mM.

Instrument Design. The design of the electron spin echo spectrometer has been described previously (Britt et al., 1989). The time resolution of the instrument has been improved to 1 ns by using Stanford Research Systems DG535 digital delay generators, and a four-step phase cycling routine is now used in three-pulse ESEEM experiments to reduce the instrumental dead time and eliminate unwanted two-pulse echoes (Fauth et al., 1986). ESEEM data recorded at a microwave frequencies near 9.2 GHz were obtained with samples in EPR tubes inserted into a waveguide-mounted loop-gap resonator probe structure (Britt & Klein, 1987). The ESEEM data recorded at frequencies near 8.5 GHz were obtained with samples loaded into the Teflon cell of a strip-line transmission cavity similar to that described by Mims and Peisach (1976). All experiments reported were performed at a temperature of 4.2 K.

Results and Discussion

(1) The Rieske Fe–S Centers Are Each Coordinated by Two Distinct Classes of Nitrogen Ligands. The ESEEM method is a pulsed EPR technique used to measure transitions of paramagnetic nuclei magnetically coupled to electron spins. Electron spin echoes are formed by the application of two or more resonant microwave pulses. In addition to inducing the electron spin transitions, the microwave pulses may also induce "semiforbidden" transitions of paramagnetic nuclear moments magnetically coupled to the electron spins, resulting in quantum-mechanical coherences in the nuclear spin sublevels associated with the electron spin levels. These coherences create interference effects that can be measured by varying the electron spin echo pulse timings (Mims, 1972a,b). Fourier analysis of the resulting electron spin echo envelope modulation (ESEEM) pattern reveals the frequencies of the various nuclear transitions. These frequencies can then be interpreted to determine superhyperfine and electric quadrupolar couplings. Details of experimental and theoretical aspects of the use of the ESEEM technique are provided in several review articles (Mims, 1972c; Kevan, 1979; Mims & Peisach, 1981; Thomann et al., 1984.

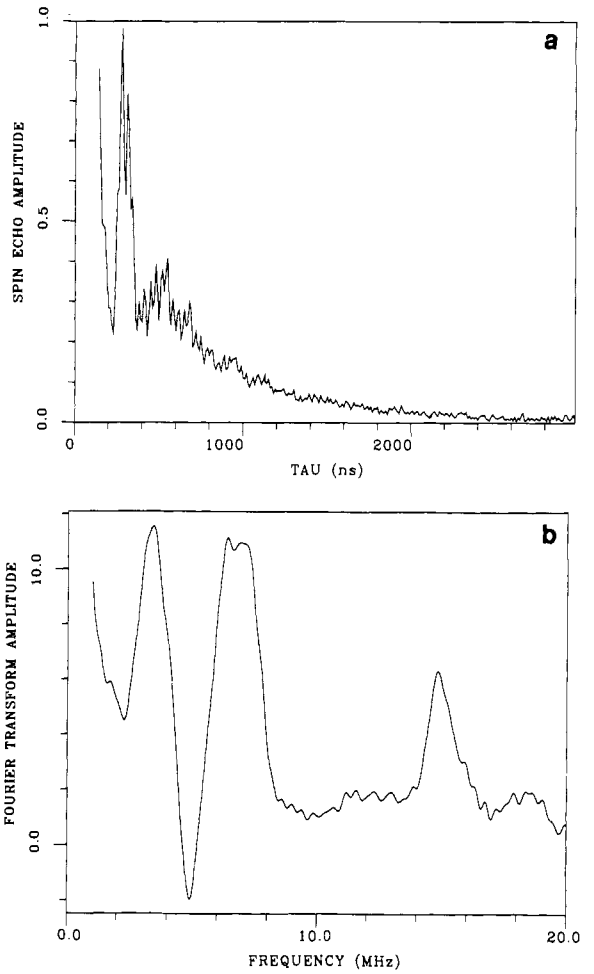

FIGURE 1: Two-pulse ESEEM pattern (a, top) and cosine Fourier transform (b, bottom) obtained at the $g = 1.92$ maximum of the Rieske ESE signal of the cytochrome b_6f complex isolated from spinach. The time τ between microwave pulses I and II was incremented in 10-ns steps between 140 and 3000 ns. The data were recorded at a temperature of 4.2 K, a microwave frequency of 9.2160 GHz, and a magnetic field of 3.460 kG. The repetition time between pulse sets was 10 ms.

Figure 1 displays the two-pulse ESEEM pattern obtained for the cytochrome b_6f complex isolated from spinach. The ESEEM results are obtained at the $g = 1.92$ maximum of the Rieske ESE signal. This field position minimizes ESEEM contributions from any underlying cytochrome signals. The two-pulse data shown in Figure 1a are obtained by recording the ESE amplitude as a function of the time τ between microwave pulses I and II. Figure 1b displays the cosine Fourier transform of the time domain pattern. The short experimental

deadtime is reconstructed by a Fourier back-fill method (Mims, 1984). The cosine Fourier transform displays the nuclear transition frequencies for paramagnetic nuclei coupled to the electron spin of the Fe–S cluster. Sum and difference frequencies may also appear in the two-pulse ESEEM Fourier transform. The peak at 14.8 MHz in Figure 1b is the "matrix" proton line that results from weakly coupled protons in the vicinity of the cluster. The broad peaks at 3.2 and 6.8 MHz arise potentially from ^{14}N nuclei.

The frequency resolution of the two-pulse ESEEM experiment displayed in Figure 1 is limited by the short-phase memory ($T_M \approx 350$ ns), which describes the overall decay of the spin echo apart from the effects of nuclear modulation. The resolution limit imposed by a short-phase memory is eliminated by employing a three-pulse "stimulated echo" sequence. In a three-pulse ESEEM experiment, the time τ between pulses I and II is held fixed, and the time T between pulses II and III is varied, while recording the amplitude of the stimulated echo that occurs at time τ after pulse III. The frequencies obtained by Fourier analysis with the time variable ($\tau + T$) consist of only fundamental nuclear transition frequencies. Sum and difference frequencies are eliminated. However, partial suppression of frequencies may occur at certain values of τ. Figure 2a displays the three-pulse ESEEM pattern for the Rieske center of the cytochrome b_6f complex of spinach. The cosine Fourier transform is displayed in Figure 2b. The frequency range is changed to only cover the 0–10-MHz range in order to examine more closely the low-frequency transitions. The increased resolution of the three-pulse experiment is observed in the splitting of the higher frequency peak into two transitions at 6.36 and 7.14 MHz.

Similar three-pulse ESEEM patterns are observed with the Rieske centers of the cytochrome bc_1 complexes. Figure 3a displays the cosine Fourier transform of the three-pulse ESEEM of the Rieske Fe–S center of the cytochrome bc_1 complex isolated from *R. rubrum*. There is a broad feature between 3 and 4 MHz and a pair of peaks at 6.32 and 7.27 MHz. The corresponding data from *R. sphaeroides* are displayed in Figure 3b. The two high-frequency peaks are at 6.38 and 7.33 MHz. The cosine Fourier transform of the three-pulse ESEEM of the bovine heart mitochondrial Rieske center is shown in Figure 3c, with high-frequency peaks at 6.31 and 7.34 MHz.

The ESEEM results obtained from the Rieske Fe–S centers are very different from the ESEEM results obtained from 2Fe–2S centers with only diamagnetic ^{32}S ligands from protein cysteine residues. An example of such a "conventional" 2Fe–2S center is the water-soluble, spinach chloroplast ferredoxin. The two- and three-pulse ESEEM results obtained with this 2Fe–2S center are displayed in Figures 4 and 5. Several transitions are observed in the frequency range below 5 MHz. Similar ESEEM patterns have been observed in several Fe–S centers (LoBrutto et al., 1987; Cammack et al., 1988). Cammack et al. (1988) have determined that these modulation components most likely arise from a single peptide nitrogen with a weak superhyperfine coupling ($A \approx 1.1$ MHz) to the unpaired spin of the Fe–S cluster. An X-ray determined structure of plant ferredoxin from *Spirulina platensis* demonstrates the presence of hydrogen bonding between peptide nitrogen atoms and the bridging sulfur atoms (Tsukihara et al., 1981). The magnetic coupling evidenced in the ESEEM patterns is most likely introduced by these hydrogen bonds. The maximum frequency attributable to ^{14}N transitions in the spinach ferredoxin is at 4.35 MHz. We have observed that the Fourier transforms of the three-pulse ESEEM patterns

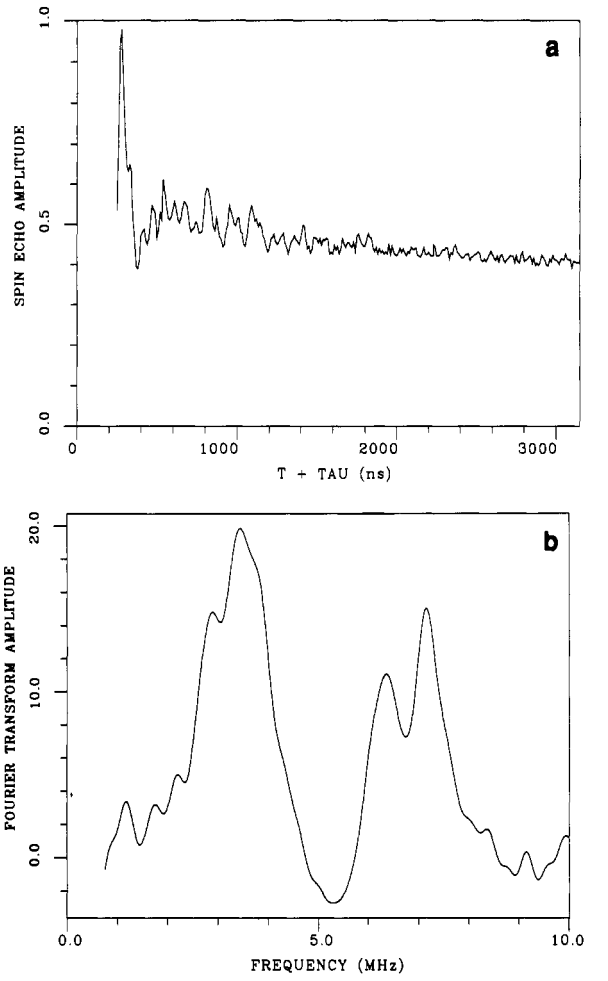

FIGURE 2: Three-pulse ESEEM pattern (a, top) and cosine Fourier transform (b, bottom) obtained at the $g = 1.92$ maximum of the Rieske ESE signal of the cytochrome b_6f complex isolated from spinach. The time τ between microwave pulses I and II was held fixed at 170 ns, while the time T between pulses II and III was incremented in 10-ns steps between 80 and 3000 ns. The data were recorded at a temperature of 4.2 K, a microwave frequency of 9.2277 GHz, and a magnetic field of 3.463 kG. The repetition time between pulse sets was 10 ms.

of each of the Rieske Fe–S centers contain a pair of peaks in the 6–8-MHz range.[2] We can tentatively assign these components to ^{14}N nuclei with stronger superhyperfine couplings than observed in the case of spinach ferredoxin.

In order to rigorously assign these transitions to nitrogen ligands, we have repeated the Rieske ESEEM measurements at a different microwave frequency and magnetic field, keeping the effective g value constant at $g = 1.92$. We thus vary only the Larmor frequency $\nu_i = g_n\mu_nB_0$ for the ^{14}N ligands. The superhyperfine and electric quadrupole couplings remain unvaried, and by working at the same g value we select the same set of orientations in the resulting powder pattern. The results for the Rieske center of the spinach cytochrome b_6f complex are shown in Figure 6, which displays the cosine Fourier transform of the three-pulse ESEEM pattern at a microwave frequency of 8.5460 GHz and a magnetic field of 3207 G. The pair of high-frequency resonances occur at 6.26 and 7.02 MHz.

[2] Previously published ESEEM results of the Rieske Fe–S centers from *T. thermophilus* (Cline et al., 1985) and yeast mitochondrial complex III (Telser et al., 1987) have shown only one peak in this frequency range. This is a result of the large values of τ employed (252 and 278 ns) in those experiments. We observe similar results in the cytochrome b_6f and cytochrome bc_1 complexes with correspondingly large values of τ.

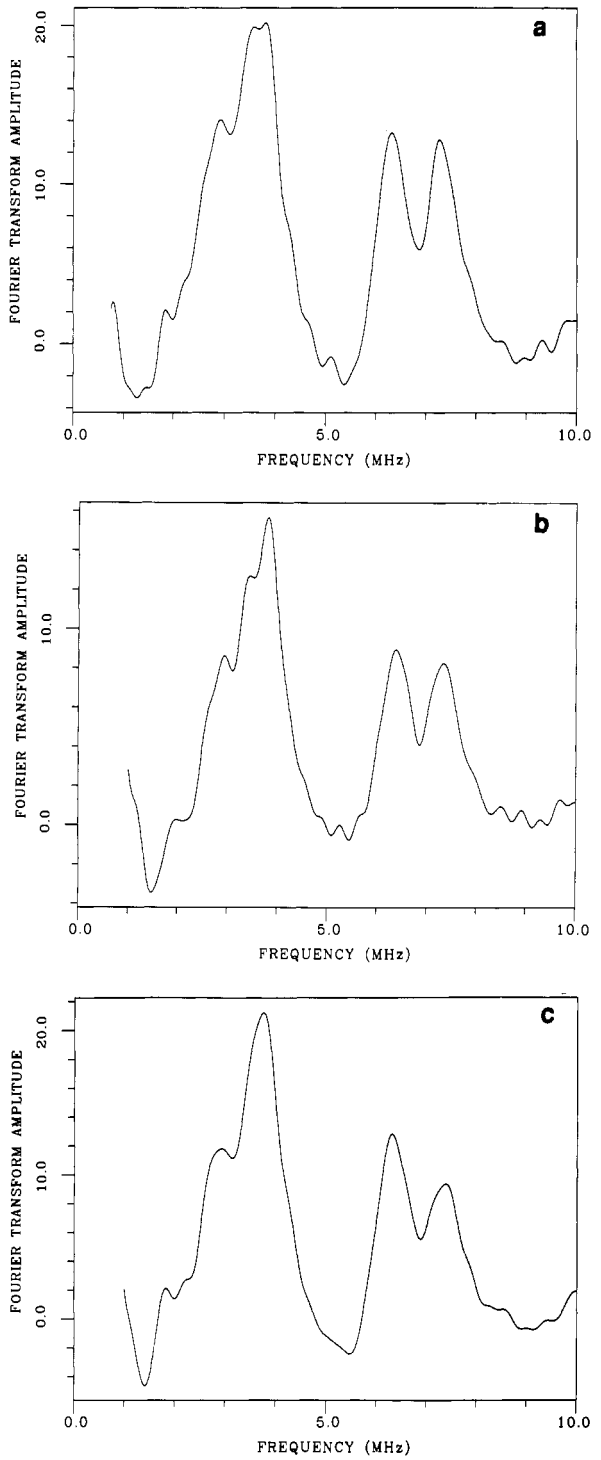

FIGURE 3: Cosine Fourier transform of the three-pulse ESEEM pattern obtained at the $g = 1.92$ maximum of the Rieske ESE signal of the cytochrome bc_1 complexes of (a, top) *Rhodospirillum rubrum*, (b, middle) *Rhodobacter sphaeroides* R-26, and (c, bottom) bovine heart mitochondria. The time τ between microwave pulses I and II was held fixed at 170 ns, while the time T between pulses II and III was incremented in 10-ns steps between 80 and 3000 ns. The data were recorded at a temperature of 4.2 K, a microwave frequency of 9.2277 GHz, and a magnetic field of 3.463 kG [(a) and (b)] and 3.465 kG (c). The repetition time between pulse sets was 10 ms.

The lower frequency peak appears to be split into two transitions at 3.10 and 3.63 MHz. The ^{14}N Larmor frequency is $\nu_i = 0.984$ MHz at this field. These results can be compared to the cytochrome b_6f ESEEMs of Figure 2, which were recorded at a microwave frequency of 9.2277 GHz and a magnetic field of 3463 G, corresponding to a Larmor frequency of $\nu_i = 1.06$ MHz.

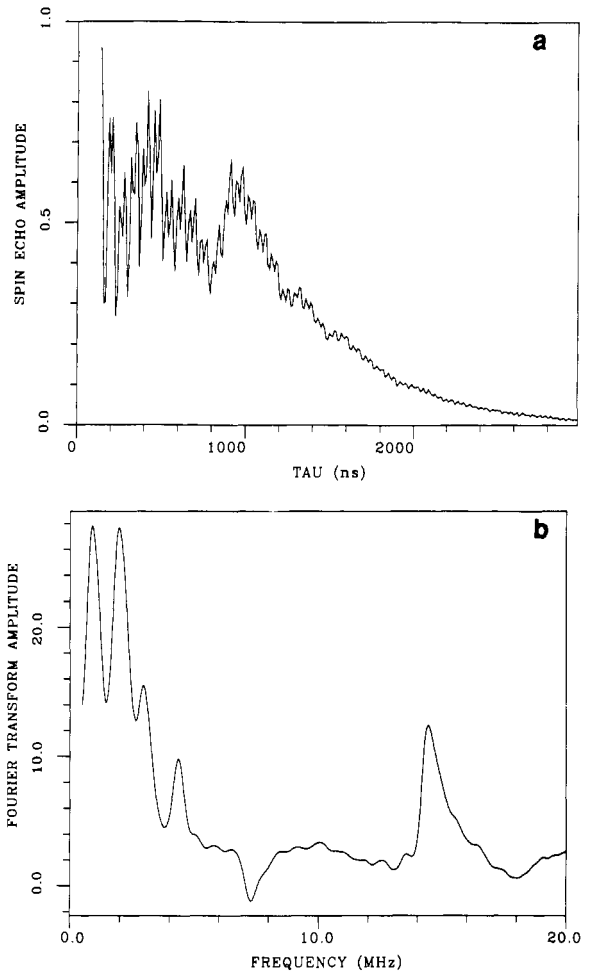

FIGURE 4: Two-pulse ESEEM pattern (a, top) and cosine Fourier transform (b, bottom) obtained at the $g = 1.96$ maximum of the ESE signal of the water-soluble ferredoxin isolated from spinach chloroplasts. The time τ between microwave pulses I and II was incremented in 10-ns steps between 140 and 3000 ns. The data were recorded at a temperature of 4.2 K, a microwave frequency of 9.2277 GHz, and a magnetic field of 3.370 kG. The repetition time between pulse sets was 50 ms.

A paramagnetic nucleus with a hyperfine interaction with a $S = {}^1/_2$ electron spin is subjected to one of two effective magnetic fields that result from the vector summation of the applied magnetic field and the hyperfine field from each electron spin orientation. In the simplest analysis, we consider the electron spin to be quantized along the direction of the applied field, resulting in colinear hyperfine and applied magnetic fields if we further approximate the hyperfine coupling to be isotropic. The magnitudes of the two effective fields can be expressed as

$$\nu_{ef}^{-} = \left|\nu_i - \frac{|A|}{2}\right| \qquad \nu_{ef}^{+} = \left|\nu_i + \frac{|A|}{2}\right| \tag{1}$$

where ν_i is the nuclear Larmor frequency due to the external applied field and A is the isotropic hyperfine coupling constant. A spin $I = 1$ nucleus such as ^{14}N also has an electric quadrupole moment that interacts with the electric field gradient at the site of the nucleus. We denote the principal values of the electric field gradient as $V_{xx} \equiv eq_{xx}$, $V_{yy} \equiv eq_{yy}$, and $V_{zz} \equiv eq_{zz}$, with the ordering of the principal axes chosen such that $|q_{xx}| \leq |q_{yy}| \leq |q_{zz}|$. For the $I = 1$ ^{14}N nucleus, the quadrupolar Hamiltonian $\mathcal{H}_Q$ may then be written:

$$\mathcal{H}_Q = \frac{e^2qQ}{4}[3I_z^2 + I^2 + \eta(I_x^2 - I_y^2)] \tag{2}$$

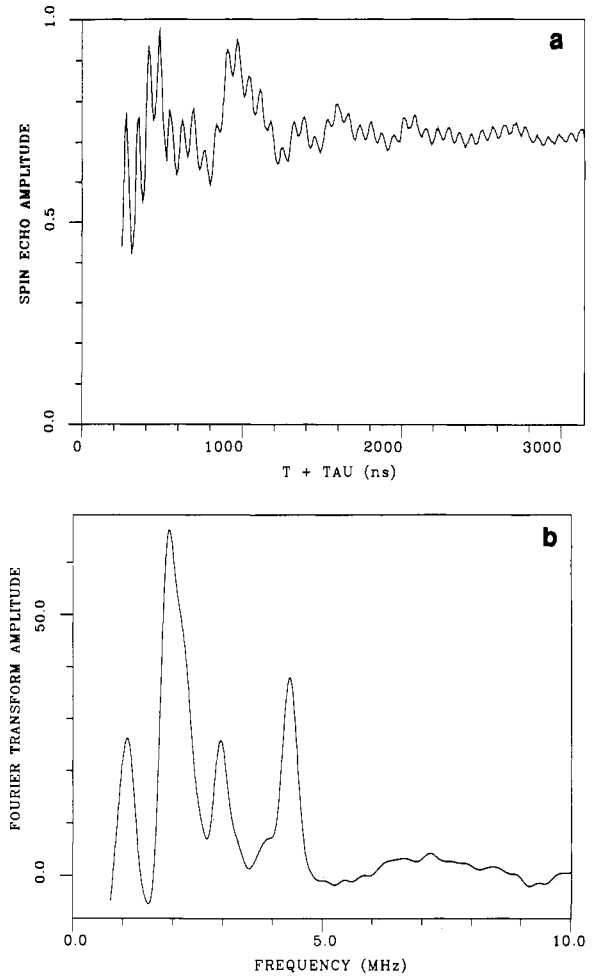

FIGURE 5: Three-pulse ESEEM pattern (a, top) and cosine Fourier transform, (b, bottom) obtained at the $g = 1.96$ maximum of the ESE signal of the water-soluble ferredoxin isolated from spinach. The time τ between microwave pulses I and II was held fixed at 170 ns, while the time T between pulses II and III was incremented in 10-ns steps between 80 and 3000 ns. The data were recorded at a temperature of 4.2 K, a microwave frequency of 9.2277 GHz, and a magnetic field of 3.370 kG. The repetition time between pulse sets was 100 ms.

where Q is defined as the scalar quadrupole moment for the the ^{14}N nucleus, $q \equiv q_{zz}$, and the asymmetry parameter η is defined by

$$\eta = \left|\frac{q_{xx} - q_{yy}}{q_{zz}}\right| \tag{3}$$

In order to assign the ESEEM frequencies observed for the Rieske Fe–S center, it is necessary to calculate the effects of both the electric quadrupole and magnetic dipole terms. The Hamiltonian for the $I = 1$ ^{14}N nucleus with electric quadrupole parameters e^2qQ and η in a magnetic field of magnitude ν_{ef} oriented with spherical angles θ and ϕ relative to the quadrupolar principal axes (x, y, z) can be written (Casabella & Bray, 1958) as in eq 4.

$$\mathcal{H} = \begin{pmatrix} \frac{e^2qQ}{4}(1+\eta) & \nu_{ef}\sin\theta\cos\varphi & \nu_{ef}\cos\theta \\ \nu_{ef}\sin\theta\cos\varphi & -\frac{e^2qQ}{2} & -i\nu_{ef}\sin\theta\sin\varphi \\ \nu_{ef}\cos\theta & i\nu_{ef}\sin\theta\sin\varphi & \frac{e^2qQ}{4}(1-\eta) \end{pmatrix} \tag{4}$$

For a given effective field and orientation parameters θ and ϕ, the Hamiltonian of eq 4 can be diagonalized to yield three energy levels with three resultant transition frequencies. Since

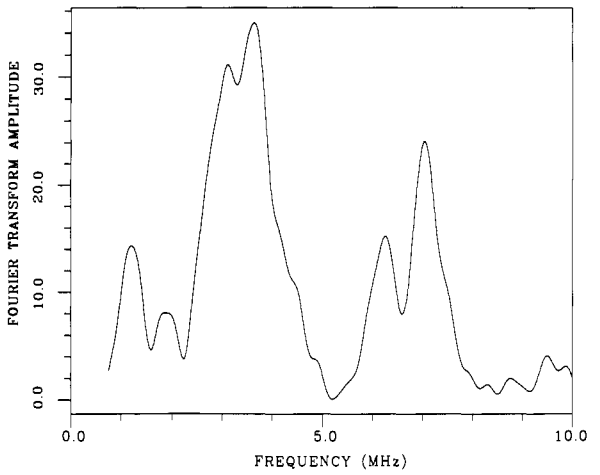

FIGURE 6: Cosine Fourier transform of the three-pulse ESEEM pattern obtained at the $g = 1.92$ maximum of the Rieske ESE signal of the cytochrome b_6f complex isolated from spinach. These data were recorded at a microwave frequency of 8.5460 GHz and a magnetic field of 3.207 kG. The time τ between microwave pulses I and II was held fixed at 147 ns, while the time T between pulses II and III was incremented in 10-ns steps between 80 and 3000 ns. The repetition time between pulse sets was 10 ms.

there are two effective field values for a nucleus subjected to both external and hyperfine fields, there is a total of six ^{14}N transition frequencies. However, unless the ESEEM experiment is performed at a field corresponding to one of the two extreme g values, the observed ESEEM patterns result as a powder pattern average of a band of values of θ and ϕ. The two "single-quantum" transitions between the inner level and the upper and lower levels can be very broad in a powder pattern average. However, the "double-quantum" transition between the upper and lower levels remains sharp in a powder pattern average. This can be readily seen by using a graphical analysis method (Astashkin et al., 1984; Flanagan & Singel, 1987) akin to that developed for analyzing triplet EPR spectra (Kottis & Lefebvre, 1963). The condition that two of the three roots of the secular equation resulting from the Hamiltonian of eq 4 be separated by frequency ν can be written in the simple form

$$F(\nu) = g(\theta,\phi) \tag{5}$$

where the angle dependence is all expressed in the term

$$g(\theta,\phi) = 3\cos^2\theta + \eta\cos 2\phi\sin^2\theta - 1 \tag{6}$$

and the resonance frequency ν is contained in the frequency-normalized term

$$F(\nu) = 2^{-3}(e^2qQ)^2\nu_{ef}^{-2}(1-\eta^2) \pm 2^2 3^{-3/2}\nu_{ef}^{-2}(e^2qQ)^{-1}[\nu^2 - \nu_c^2][4\nu_c^2 - \nu^2]^{1/2} \tag{7}$$

with

$$\nu_c \equiv [\nu_{ef}^2 + 2^{-4}(3+\eta^2)(e^2qQ)^2]^{1/2} \tag{8}$$

The function $F(\nu)$ can be plotted as shown in part a of Figure 7 for ν_{ef}^+ and part b for ν_{ef}^-. For a given effective field ν_{ef}, the three transition frequencies for specified angles θ and ϕ are determined by the values of the frequency ν at which the function $g(\theta,\phi)$ equals $F(\nu)$. The value of $g(\theta,\phi)$ ranges from a minimum $(-1 - \eta)$, with the magnetic field oriented along the electric field gradient principal axis x, to a maximum $(+2)$ for the magnetic field parallel to the axis z. The two single-quantum transitions occur in the frequency range delimited by ν_1 and ν_2 in Figure 7a,b. The double-quantum transitions occur within the narrower frequency range between ν_3 and ν_4. Figure 7c displays the cosine Fourier transform of a simulated

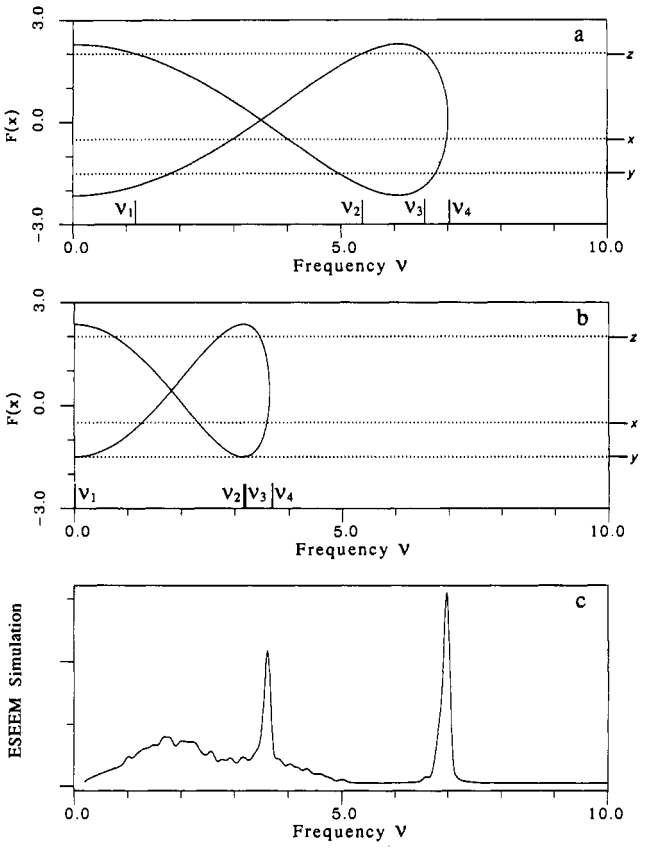

FIGURE 7: Graphical analysis of ^{14}N transition frequencies. Parts a and b show plots of the function $F(\nu)$ versus frequency (ν). Resonances occur at the frequencies ν where the function $g(\theta,\phi) = 3\cos^2\theta + \eta\cos 2\phi \sin^2\theta - 1$ intersects the two branches of $F(\nu)$. The curves are generated with the parameters $e^2qQ = 2.8$ MHz, $n = 0.5$, $A = 4.58$ MHz, and $\nu_i = 0.98$ MHz (3207 G). The curve in (a) is generated for $\nu_{ef}^+ = A/2 + \nu_i$. The curve in (b) is generated for $\nu_{ef}^- = A/2 - \nu_i$. The double-quantum transitions occur in a narrow frequency band with upper bound $2\nu_c = \nu_{dq} = 2[\nu_{ef}^2 + (e^2qQ)^2(3 + \eta^2)/16]^{1/2}$. The lower band is determined by the lowest frequency intersect of $F(\nu)$ within the band $(-1 - \eta) < g(\theta,\phi) < 2$. The single-quantum transitions occur over a much broader frequency range and are often not observed in the ESEEM experiment. Part c shows the three-pulse ESEEM simulation ($\tau = 147$ ns) constructed with the same parameters. The two double-quantum peaks occur at 3.6 and 7.0 MHz and match with two of the four ESEEM transitions observed in Figure 6. The simulation methods are described by Britt et al. (1989).

three-pulse powder pattern ESEEM spectrum. The double-quantum transitions give rise to the two well-resolved peaks, and the single-quantum transitions appear as a broad low-frequency feature. The maximum frequency for the double-quantum transition is determined by the high-frequency intersection $\nu_4 = 2\nu_c$ of two branches of the function $F(\nu)$. The ESEEM amplitudes in a powder pattern average are weighted toward the high-frequency limit (Flanagan & Singel, 1987), and to good approximation the frequencies of the two double-quantum transitions corresponding to the two fields ν_{ef}^+ and ν_{ef}^- can be written as

$$\nu_{dq}^{\pm} = 2\left[\left|\nu_i \pm 1/2\left|A\right|\right|^2 + \xi^2\right]^{1/2} \quad (9)$$

with the quadrupolar parameters e^2qQ and η contained in the term

$$\xi = \frac{e^2qQ}{4}(3 + \eta^2)^{1/2} \quad (10)$$

The ESEEM features of the Rieske center of the cytochrome b_6f complex exhibit a decrease in the frequencies of the transitions between 3 and 4 MHz as the magnetic field is increased. Such a decrease in frequency with increased field can result only from a decrease in the effective field ν_{ef}^- in the limit where $|A|/2 > \nu_i$. The features between 6 and 7 MHz increase in frequency with increased field, and they correspond to the effective field ν_{ef}^+. We thus assign the four transitions observed in Figure 6 to result from two classes of inequivalent ^{14}N ligands with both classes in the magnetic field regime such that $|A|/2 > \nu_i$.

The remaining ambiquity in assigning specific coupling parameters to the two classes arises from the two different possible pairings for the ν_{dq}^+ and ν_{dq}^- transitions for each of the two classes. For example, we can suppose that the transitions at 3.63 and 6.26 MHz result from one class of ^{14}N ligand and the transitions at 3.10 and 7.02 MHz result from the other class. We can use eq 9 to calculate the values of A and ξ for each class. The proposed class with transitions at 3.63 and 6.26 MHz would then have a hyperfine coupling of $A = 3.31$ MHz. The quadrupolar parameter would be $\xi = 1.68$ MHz, and allowing the asymmetry parameter η to vary between 0 and 1 gives a range of values for the coupling constant e^2qQ between 3.36 and 3.87 MHz. This is a rather large coupling constant for a ^{14}N in a protein environment [as reviewed by Edmonds (1977)]. NQR measurements of peptide nitrogens in dipeptide and tripeptide compounds demonstrate a range of e^2qQ values between 3.0 and 3.4 MHz (Edmonds & Speight, 1971; Hunt & Mackay, 1976). The only other protein ^{14}N site with equivalently large couplings is the imino nitrogen of the imidazole ring of histidine ($e^2qQ = 3.36$ MHz), though the value of this coupling constant is reduced upon coordination to metals (Ashby et al., 1978). The other potential class of ^{14}N arising from this pairing assignment would have transitions at 3.10 and 7.02 MHz and describes a site yet more unlikely. The hyperfine coupling for such a site would be 5.06 MHz, and the quadrupolar parameter ξ would be 0.0 MHz, forcing the quadrupolar coupling e^2qQ to be equal to zero. We consider it very unlikely that the electric field gradient at a nitrogen at the Rieske center would be zero. Because of the very high and incredibly low value of e^2qQ forced by this pairing of the four peaks, we consider this pairing assignment to be incorrect.

We believe the correct assignment results by pairing the two peaks at 3.63 and 7.02 MHz and considering them to result from the two double-quantum transitions from one class of ^{14}N ligand. The resulting parameters are $A_1 = 4.58$ MHz and $\xi_1 = 1.26$ MHz. The remaining two features at 3.10 and 6.26 MHz then result as the two double-quantum transitions from another class of ^{14}N ligands with $A_2 = 3.75$ MHz and $\xi_2 = 1.27$ MHz. The value of the asymmetry parameter η is not uniquely determined in these ESEEM measurements.[3] However, by varing η from 0 to 1 we can determine that the electric quadrupole coupling parameter e^2qQ for each of the two nitrogen classes is between 2.5 and 2.9 MHz. We note that this is within the range expected for the imino nitrogen of imidazole coordinated to a metal ion. Ashby et al. (1978) measured the ^{14}N NQR spectra of the imino nitrogen in a series of zinc and cadmium complexes of imidazole, and the e^2qQ values of these metal-coordinated nitrogens ranged be-

[3] ESEEM experiments performed at a field position such that $|A|/2 \approx \nu_i$ can reveal the zero-field splittings for a ^{14}N nucleus coupled to an electron spin (Mims & Peisach, 1978). The two parameters e^2qQ and η can be determined directly from these zero-field splittings. However, the values of the couplings to the two classes of nitrogens would require working at microwave frequencies above the range of our X-band instrument in this case.

tween 1.96 and 2.82 MHz. Also, we note that the magnitude of the hyperfine couplings $A_1 = 4.58$ and $A_2 = 3.75$ MHz for our two classes of nitrogens are approximately four times greater than the $A = 1.1$ MHz coupling to the peptide nitrogen that gives rise to the modulation patterns of spinach ferredoxin in Figures 4 and 5. We consider this strong evidence that both classes of nitrogen are directly coordinated to the Rieske Fe–S clusters. The ESEEM rsults of the Rieske center of the three cytochrome bc_1 complexes displayed in Figure 3 are nearly identical with those from the cytochrome b_6f complex, and thus we consider the coordination environment to be very similar in each of these Rieske Fe–S centers. In summary, the results of our ESEEM experiments and analyses indicate that two distinct classes of nitrogens are ligated to the Rieske Fe–S clusters in the cytochrome b_6f and cytochrome bc_1 complexes, with superhyperfine couplings of approximately 4.6 and 3.8 MHz and with quadrupolar couplings in the range 2.5–2.9 MHz.

It is of course interesting to compare these results to those obtained via ENDOR on the Rieske center of the phthalate dioxygenase enzyme (Gurbiel et al., 1989). The isotropic components of the ^{15}N hyperfine couplings obtained from the ENDOR data for the two ^{15}N ligands are 6 and 7.7 MHz. These scale to 4.2 and 5.5 MHz for the isotropic hyperfine couplings for ^{14}N. The quadrupole P tensor principal values reported correspond to values of $e^2qQ = 2.6$ MHz for the first ^{14}N site and $e^2qQ = 2.3$ MHz for the second. We observe a close match between these ENDOR-derived results for the phthalate dioxygenase enzyme and the results that we have obtained via the ESEEM technique on the Rieske Fe–S clusters in the cytochrome b_6f and cytochrome bc_1 complexes.[4] We therefore consider our results to provide strong evidence that the proposed model of Gurbiel et al. (1989) for coordination of two histidines to the Fe(II) of the Rieske cluster of the phthalate dioxygenase enzyme is indeed also valid for the Rieske clusters of these oxidoreductase enzymes.

Finally, we note that the modulation components observed in spinach ferredoxin are absent from the Rieske Fe–S center results. The features in the Rieske ESEEM in the 3–4-MHz range decrease in frequency with increased field, showing that this modulation results solely from the strongly coupled nitrogens. There is no evidence of the large well-resolved peaks in the 1–4-MHz range that arise from a peptide nitrogen with a weak interaction with the unpaired spin of the Fe–S cluster. This indicates that the interaction between the Fe–S cluster and any adjacent peptide nitrogens is rather different from that in a number of Fe–S clusters with all cysteine ligands.

(2) *The Effect of DBMIB Treatment on the Rieske ESEEM Patterns.* DBMIB inhibits cytochrome b_6f function, presumably by acting as a nonfunctional analogue to plastoquinone (Trebst et al., 1970). DBMIB treatment of cytochrome b_6f preparations results in an upward shift in g values and an alteration of the midpoint potential of the Fe–S center (Malkin, 1981a,b, 1982). The DBMIB-altered EPR signal has a center g value of 1.95, and the EPR signal more closely resembles that of ferredoxins with all cysteine ligands than that of the untreated Rieske complex. Therefore, it is possible that DBMIB inhibition affects the ligation of histidines to the Rieske Fe–S center.

We have examined the DBMIB-altered Rieske center by two- and three-pulse ESEEM at microwave frequencies of 8.5962 and 9.2291 GHz. The DBMIB treatment induces a complete conversion of the Rieske EPR signal to a form with an ESE maximum at $g = 1.95$. Figure 8 displays the three-pulse ESEEM time domain pattern (a) and cosine Fourier transform (b) obtained at 9.2291 GHz with a 3381-G magnetic field. The Fourier transform shows two peaks at 6.28 and 7.07 MHz and a broad transition in the 3–4-MHz range. These peaks are very similar to those observed in the untreated Rieske center (Figure 2). The shifts in the Fourier peak positions observed at the lower field position (3150 G for a frequency of 8.5962 GHz) are also similar to those observed for the native center. We therefore have determined that the two histidine ligands are still coordinated to the center after DBMIB treatment, even though the EPR spectrum resembles that of a conventional ferredoxin. In addition, there is little change in the magnitudes of the magnetic couplings between the unpaired spin of the Fe–S cluster and the two nitrogen nuclei of the imidazole groups.

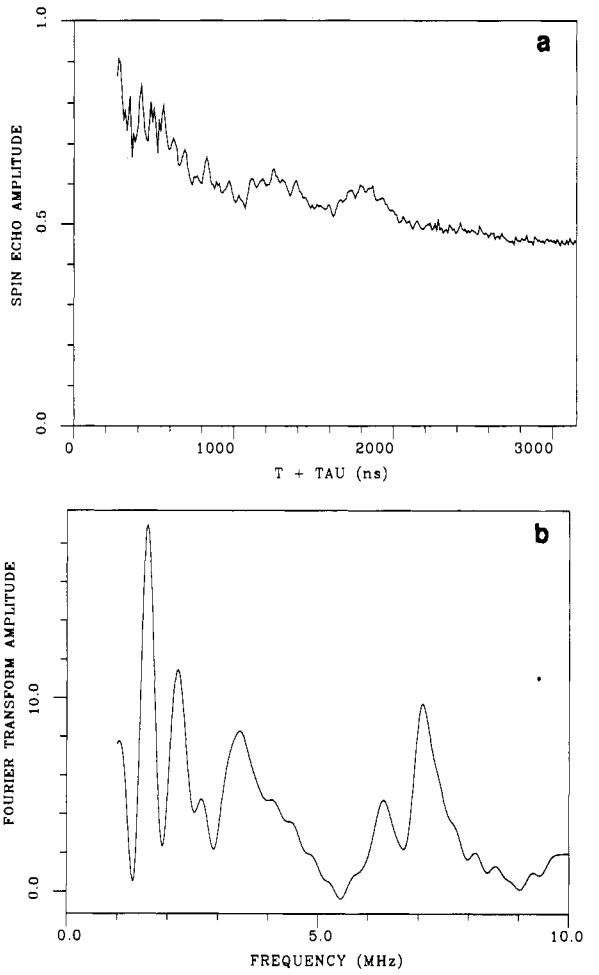

FIGURE 8: Three-pulse ESEEM pattern (a, top) and cosine Fourier transform (b, bottom) obtained at the $g = 1.95$ maximum of the DBMIB-altered Rieske ESE signal of the cytochrome b_6f complex isolated from spinach. The time τ between microwave pulses I and II was held fixed at 170 ns, while the time T between pulses II and III was incremented in 10-ns steps between 100 and 3000 ns. The data were recorded at a temperature of 4.2 K, a microwave frequency of 9.2291 GHz, and a magnetic field of 3.381 kG. The repetition time between pulse sets was 10 ms.

Additional low-frequency components are observed in the Fourier transform of the DBMIB-treated Rieske centers. The sharp features at 1.6 and 2.2 MHz are similar to features observed from peptide nitrogen in the spinach ferredoxin. These features are not present in the ESEEM patterns of the untreated Rieske center. DBMIB inhibition may induce a change in the folding pattern of the peptide about the cluster

[4] The small difference in our hyperfine and quadrupole coupling parameters may be due to our neglecting the effects of hyperfine anisotropy in the analysis of the ESEEM results.

that affects the magnitude of magnetic couplings between the unpaired electron spin and the peptide nitrogens. It is interesting to note that ferredoxin and the DBMIB-altered Rieske EPR spectra have similar g values and comparable interactions with peptide nitrogens, while the untreated Rieske centers have very different g values and no observable magnetic interaction with peptide nitrogen. This raises the possibility that the pattern of hydrogen bonds about the Fe–S cluster are important in determining the precise g values of the Fe–S EPR spectra.

ACKNOWLEDGMENTS

We thank Dr. James Fee and Dr. David Ballou for providing prepublication manuscripts of their ENDOR study of the phthalate dioxygenase Rieske center.

Registry No. L-His, 71-00-1.

REFERENCES

Ashby, C. I. H., Cheng, C. P., & Brown, T. L. (1978) *J. Am. Chem. Soc. 100*, 6057–6063.

Astashkin, A. V., Dikanov, S. A., & Tsvetkov, Y. D. (1984) *J. Struct. Chem. 25*, 45–55.

Beckmann, J. D., Ljungdahl, P. O., Lopez, J. L., & Trumpower, B. L. (1987) *J. Biol. Chem. 262*, 8901–8909.

Bertrand, P., Guigliarelli, B., Gayda, J.-P., Beardwood, P., & Gibson, J. F. (1985) *Biochim. Biophys. Acta 831*, 261–266.

Blumberg, W. E., & Peisach, J. (1974) *Arch. Biochem. Biophys. 162*, 502–512.

Britt, R. D., & Klein, M. P. (1987) *J. Magn. Reson. 74*, 535–540.

Britt, R. D., Zimmerman, J.-L., Sauer, K., & Klein, M. P. (1989) *J. Am. Chem. Soc. 111*, 3522–3532.

Buchanan, B. B., & Arnon, D. I. (1971) *Methods Enzymol. 23*, 413–440.

Cammack, R., Chapman, A., McCracken, J., Cornelius, J. B., Peisach, J., & Weiner, J. H. (1988) *Biochim. Biophys. Acta 956*, 307–312.

Casabella, P. A., & Bray, P. J. (1958) *J. Chem. Phys. 28*, 1182–1187.

Cline, J. F., Hoffman, B. M., Mims, W. B., LaHaie, E., Ballou, D. P., & Fee, J. A. (1985) *J. Biol. Chem. 260*, 3251–3254.

Dutton, P. L. (1986) in *Encyclopedia of Plant Physiology, New Series, Volume 19, Photosynthesis III* (Staehelin, L. A., & Arntzen, C. J., Eds.) pp 197–237. Springer-Verlag, Berlin.

Edmonds, D. T. (1977) *Phys. Rep. C 29*, 233–290.

Edmonds, D. T., & Speight, P. A. (1971) *Phys. Lett. 34A*, 325–326.

Fauth, J.-M., Schweiger, A., Braunschweiler, L., Forrer, J., & Ernst, R. R. (1986) *J. Magn. Reson. 66*, 74–85.

Fee, J. A., Findling, K. L., Yoshida, T., Hille, R., Tarr, G. E., Hearshen, D. O., Dunham, W. R., Day, E. P., Kent, T. A., & Münck, E. (1984) *J. Biol. Chem. 259*, 124–133.

Fee, J. A., Kuila, D., Mather, M. W., & Yoshida, T. (1986) *Biochim. Biophys. Acta 853*, 153–185.

Flanagan, H. L., & Singel, D. J. (1987) *J. Chem. Phys. 87*, 5606–5616.

Gabellini, N., & Sebald, W. (1986) *Eur. J. Biochem. 154*, 569–579.

Gatti, D. L., Meinhardt, S. W., Ohnishi, T., & Tzagoloff, A. (1989) *J. Mol. Biol. 205*, 421–435.

Gurbiel, R. J., Batie, C. J., Sivaraja, M., True, A. E., Fee, J. A., Hoffman, B. M., & Ballou, D. P. (1989) *Biochemistry 28*, 4861–4871.

Harnisch, U., Weiss, H., & Sebald, W. (1985) *Eur. J. Biochem. 149*, 95–99.

Hauska, G. (1986) in *Encyclopedia of Plant Physiology, New Series, Volume 19, Photosynthesis III* (Staehelin, L. A., & Arntzen, C. J., Eds.) pp 496–507. Springer-Verlag, Berlin.

Hunt, M. J., & Mackay, A. L. (1976) *J. Magn. Reson. 22*, 295–301.

Hurt, E., & Hauska, G. (1981) *Eur. J. Biochem. 117*, 591–599.

Kevan, L. (1979) in *Time Domain Electron Spin Resonance* (Kevan, L., & Schwartz, R. N., Eds.) pp 279–341, Wiley, New York.

Kottis, P., & Lefebvre, R. (1963) *J. Chem. Phys. 39*, 393–403.

Kriauciunas, A., Yu, L., Yu, C.-A., Wynn, R. M., & Knaff, D. B. (1989) *Biochim. Biophys. Acta 976*, 70–76.

Kurowski, B., & Ludwig, B. (1987) *J. Biol. Chem. 262*, 13805–13811.

LoBrutto, R., Haley, P. E., Yu, C.-A., & Ohnishi, T. (1987) *Adv. Membr. Biochem. Bioenerg.*, 499–458.

Malkin, R. (1981a) *FEBS Lett. 131*, 169–172.

Malkin, R. (1981b) *Isr. J. Chem. 21*, 301–305.

Malkin, R. (1982) *Biochemistry 21*, 2945–2950.

Mims, W. B. (1972a) *Phys. Rev. B 5*, 2409–2419.

Mims, W. B. (1972b) *Phys. Rev. B 6*, 3543–3545.

Mims, W. B. (1972c) in *Electron Paramagnetic Resonance* (Geschwind, S., Ed.) pp 263–351, Plenum Press, New York.

Mims, W. B. (1984) *J. Magn. Reson. 59*, 291–306.

Mims, W. B., & Peisach, J. (1976) *Biochemistry 15*, 3863–3869.

Mims, W. B., & Peisach, J. (1978) *J. Chem. Phys. 69*, 4921–4930.

Mims, W. B., & Peisach, J. (1981) in *Biological Magnetic Resonance* (Berliner, L. J., & Reuben, J., Eds.) Vol. 3, pp 213–263, Plenum Press, New York.

Mitchell, P. (1975) *FEBS Lett. 56*, 1–6.

Mitchell, P. (1976) *J. Theor. Biol. 62*, 327–367.

Nitschke, W., & Hauska, G. (1987) in *Progress in Photosynthesis Research* (Biggins, J., Ed.) Vol. II, pp 165–172. Martinus Nijhoff Publishers, Dordrecht.

Ort, D. R. (1986) in *Encyclopedia of Plant Physiology, New Series, Volume 19, Photosynthesis III* (Staehelin, L. A., & Arntzen, C. J., Eds.) pp 143–196. Springer-Verlag, Berlin.

Powers, L, Schägger, H., von Jagow, G., Smith, J., Chance, B., & Ohnishi, T. (1989) *Biochim. Biophys. Acta 975*, 293–298.

Rieske, J. S. (1976) *Biochim. Biophys. Acta 456*, 195–247.

Rieske, J. S., Zaugg, W. S. & Hansen, R. E. (1964) *J. Biol. Chem. 239*, 3023–3030.

Schägger, H., Borchart, U., Machleidt, W., Link, T. A., & von Jagow, G. (1987) *FEBS Lett. 219*, 161–168.

Scholes, C. P., Lapidot, A., Mascarenhas, R., Inubushi, T., Isaacson, R. A., & Feher, G. (1982) *J. Am. Chem. Soc. 104*, 2724–2735.

Steppuhn, J., Rother, C., Hermans, J., Jansen, T., Salnikow, J., Hauska, G., & Herrmann, R. G. (1987) *Mol. Gen. Genet. 210*, 171–177.

Telser, J., Hoffman, B. M., LoBrutto, R., Ohnishi, T., Tsai, A.-L., Simkin, D., & Palmer, G. (1987) *FEBS Lett. 214*, 117–121.

Thomann, H., Dalton, L. R., & Dalton, L. A. (1984) in *Biological Magnetic Resonance* (Berliner, L. J., & Reuben, J., Eds.) Vol. 6, pp 143–186, Plenum Press, New York.
Trebst, A., Harth, E., & Draber, W. (1970) *Z. Naturforsch. 25b*, 1157–1159.
Tsang, H.-T., Batie, C. J., Ballou, D. P., & Penner-Hahn, J. E. (1989) *Biochemistry 28*, 7233–7240.
Tsukihara, T., Fukuyama, K., Nakamura, M., Katsube, Y., Tanaka, N., Kakudo, M., Wada, K., Hase, T., & Matsubara, H. (1981) *J. Biochem. 90*, 1763–1773.
Wikström, M., & Krab, K. (1980) *Curr. Top. Bioenerg. 10*, 51–101.
Wikström, M., Krab, K., & Saraste, M. (1981) *Annu. Rev. Biochem. 50*, 623–655.
Yu, C.-A., & Yu, L. (1980) *Biochim. Biophys. Acta 591*, 409–420.
Yu, L., Mei, Q.-C., & Yu, C.-A. (1984) *J. Biol. Chem. 259*, 5752–5760.

The 30-Kilodalton Subunit of Bovine Mitochondrial Complex I Is Homologous to a Protein Coded in Chloroplast DNA†

Stephanie J. Pilkington,‡ J. Mark Skehel, and John E. Walker*
Medical Research Council Laboratory of Molecular Biology, Hills Road, Cambridge CB2 2QH, U.K.
Received June 21, 1990; Revised Manuscript Received October 29, 1990

ABSTRACT: In cattle, 7 of the 30 or more subunits of the respiratory enzyme NADH:ubiquinone reductase (complex I) are encoded in mitochondrial DNA, and potential genes (open reading frames, orfs) for related proteins are found in the chloroplast genomes of *Marchantia polymorpha* and *Nicotiana tabacum*. Homologues of the nuclear-coded 49- and 23-kDa subunits are also coded in chloroplast DNA, and these orfs are clustered with four of the homologues of the mammalian mitochondrial genes. These findings have been taken to indicate that chloroplasts contain a relative of complex I. The present work provides further support. The 30-kDa subunit of the bovine enzyme is a component of the iron–sulfur protein fraction. Partial protein sequences have been determined, and synthetic oligonucleotide mixtures based on them have been employed as hybridization probes to identify cognate cDNA clones from a bovine library. Their sequences encode the mitochondrial import precursor of the 30-kDa subunit. The mature protein of 228 amino acids contains a segment of 57 amino acids which is closely related to parts of proteins encoded in orfs 169 and 158 in the chloroplast genomes of *M. polymorpha* and *N. tabacum*. Moreover, the chloroplast orfs are found near homologues of the mammalian mitochondrial genes for subunit ND3. Therefore, the plant chloroplast genomes have at least two separate clusters of potential genes encoding homologues of subunits of mitochondrial complex I. The bovine 30-kDa subunit has no extensive sequences of hydrophobic amino acids that could be folded into membrane-spanning α-helices, and although it contains two cysteine residues, there is no clear evidence in the sequence that it is an iron–sulfur protein.

The chloroplast genomes of the liverwort, *Marchantia polymorpha*, and the tobacco plant, *Nicotiana tabacum*, are 121 024 and 155 844 bp long, and they are thought to contain 119 and 122 different genes, respectively (Ohyama et al., 1986, 1988; Shinozaki et al., 1986). Both genomes have a duplicated region, and the large difference between the sizes of the two genomes is accounted for primarily by the lengths of these inverted DNA repeats. About 90 genes have been identified in each genome, often by homology of predicted protein sequences encoded in the chloroplast DNAs with those of known proteins (Ohyama et al., 1988). They fall broadly into two categories: those involved in transcription and translation in the chloroplast and those required for bioenergetic functions, such as photosynthetic electron transport and ATP synthesis. About 60 genes are in the former group and about 20 in the latter. In addition, seven open reading frames (orfs) in the liverwort code for protein sequences that are homologous to seven components of mitochondrial NADH:ubiquinone reductase (complex I) in mammals and other species [see Fearnley et al. (1989) for a summary]. These proteins are encoded in mitochondrial DNA and are known as subunits ND1–ND6 and ND4L (Chomyn et al., 1985, 1986). The liverwort chloroplast orfs are named *ndh*1–*ndh*6 and *ndh*4L; six homologues (*ndh*A, *ndh*B, *ndh*C, *ndh*D, *ndh*E, and *ndh*F) are also present in tobacco chloroplasts, and two tobacco open reading frames (orfs 138 and 99B) correspond to liverwort *ndh*6 if a frame shift is introduced in the tobacco DNA sequence (Ohyama et al., 1988). These unexpected findings have led to suggestions that the putative chloroplast proteins encoded in the orfs are subunits of an NADH or NADPH:plastoquinone reductase component of a chloroplast respiratory electron transport activity and that this enzyme complex will be rather closely related to the mitochondrial NADH:ubiquinone reductase complex. This view is strengthened by the recent finding that the 49- and 23-kDa subunits, both nuclear-encoded components of the mitochondrial enzyme, also have homologues encoded in orfs in both chloroplast genomes (Fearnley et al., 1989; Dupuis et al., 1991), and the orfs are both in a gene cluster that also contains four of the homologues of the mitochondrial gene products of complex I.

The work presented provides further evidence for a complex I like assembly in chloroplasts. We have determined from among the 30 or more subunits of complex I isolated from bovine heart mitochondria the primary structure of the 30-kDa subunit, a component of the simpler iron–sulfur (IP) fraction

† The nucleic acid sequence in this paper has been submitted to GenBank under Accession Number J05314.
* To whom correspondence should be addressed.
‡ Supported by a Medical Research Council research studentship.

0006-2960/91/0430-1901$02.50/0